Article

Investigating the Ground-State and Ionization Processes of Hydrogen Peroxide Dimers Using Sequentially Combined Theoretical Approaches

Published as part of Journal of Chemical Theory and Computation special issue "Computational Chemistry in the Global South: The Latin American Perspective".

José L. F. Santos, Kirk A. Peterson,* and Gabriel L. C. de Souza*
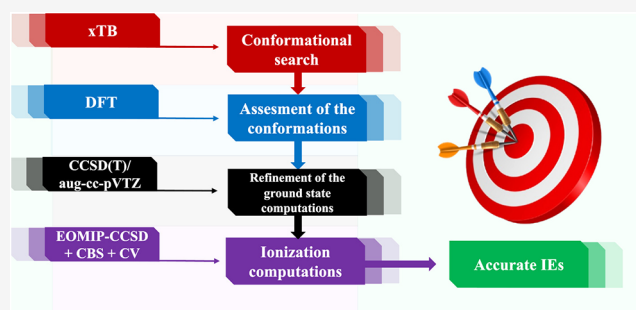
Read Online

ACCESS | Metrics & More | Article Recommendations | SI Supporting Information

ABSTRACT: We present a study of the structures and ionization energies (IEs) of a series of conformations of hydrogen peroxide (H_2O_2) dimers. Ground-state properties were computed using the coupled-cluster with single, double, and perturbative triple excitations, CCSD(T), method with large correlation-consistent basis sets, while the ten lowest-lying IEs of the H_2O_2 dimer conformations were determined through the use of the equation-of-motion ionization potential coupled-cluster with single and double excitations method (EOMIP-CCSD) combined with correlation-consistent basis sets, extrapolation to the complete basis set limit, and consideration of core-correlation effects. All of the stable conformations were determined to be within 10 kJ/mol of the most stable structure (conformation I). The first IE of conformation I was determined to be 11.72 eV, while the corresponding value for conformation V was calculated as 11.58 eV. This difference (which was also noticed for other low-lying IEs and conformations) may be helpful for the assignments of experimental results. Given that the H_2O_2 clusters were first isolated through the use of beam experiments in the recent years, it is expected that the present work can call the attention of the community. In addition, the use of the combined theoretical approaches employed regarding the selection of the relevant conformations and the exploration of the corresponding ionization processes for the molecular clusters may present an initial guide for researchers venturing into the field.

INTRODUCTION

The aggregation of small- and medium-sized molecules (through the occurrence of different types of weakly bound forces and interactions) may be assigned as a key factor in terms of providing stability and functionality to various macromolecular systems.[1−6] For example, Ozbagcr et al.[7] suggested that the binding of the fast green FCF food dye with trypsin via van der Waals interactions can lead to microenvironmental and conformational changes for this particular enzyme, while other very recent works reported such interactions as contributing to the preservation of the active sites of different enzymes.[8,9] In addition, hydrogen-bonding interactions are often associated with changes in the energetic cost of the photoexcitation processes in organic contaminants.[10−12] These play a significant role in electron scattering cross sections and the related resonances[13] and to realize the antioxidant power of polyphenolic species through the hydrogen-atom mechanism.[14,15] Therefore, it is reasonable to state that understanding the impact that the referred interactions may have on the stabilities and on different

quantities that are related to fundamental processes of molecular clusters can help in fingerprinting a part of the mysteries of the chemical and biological universe.

Peroxides are compounds that present the O−O bond as a signature in their chemical structures,[16] with hydrogen peroxide (H_2O_2) being considered the simplest compound belonging to this class. This compound is an important biomarker that may exert some interesting roles that are associated with the defense system via oxidative biosynthesis.[17−19] For instance, H_2O_2 can be generated in biological systems through oxidative burst, which involves the rapid production of a series of reactive oxygen species (ROS) in

response to the attack of a given pathogen.[20] Due to its highly oxidative power, hydrogen peroxide is considered a deleterious molecule when produced (at sufficient concentrations) in a living organism, as it can lead to cellular damage regarding either integrity or function.[21]

Beyond its ability of forming hydrogen-bonded and van der Waals complexes when interacting with chemical systems that are relevant to a variety of areas (such as atmospheric, materials, and environmental chemistry),[22−28] when in aqueous solution, H_2O_2 may engage in ion−ion interactions with other ions present in water via electrostatic forces of attraction and repulsion, often facilitated by water molecules forming so-called "water-bridged" structures.[29,30] These interactions may be used for explaining the role of carbonate speciation on the oxidation of Fe^{2+} by H_2O_2, for instance.[31] In addition, recent works suggested that H_2O_2 forms comparatively stronger hydrogen bonds with water via its hydrogen atoms than those formed between water molecules themselves,[32,33] and this observation can be attributed to hydrogen peroxide functioning as a more effective hydrogen bond donor than acceptor.[34] On the other hand, although H_2O_2−metal complexes play an important role in catalysis, materials science, and biotechnology, the characteristics of the interactions between hydrogen peroxide and metal cations are still unclear and widely debated. This uncertainty largely stems from the very low coordination strength of H_2O_2, which makes it difficult to analyze and interpret the precise nature of these interactions.[35]

From a physical-chemical standpoint, studying processes such as the detailed mechanisms of chemical reactions, electron attachment, and electron detachment happening in systems such as H_2O_2 may represent a difficult task. The challenges may originate due to the high instability of such species (being considerably difficult to be prepared as single molecules in gas-phase experiments), as well as due to their strong oxidizing nature.[36] For instance, to our knowledge, one of the few experimental investigations involving dissociative electron attachment to gas-phase H_2O_2 was carried out by Nandi et al.[37] In theory, employing molecular clusters could offer a promising strategy to overcome many of the experimental hurdles. However, it was only in 2020 that Pysanenko et al.[38] made the first attempt to produce H_2O_2 clusters through a molecular beam, which is a considerably complicated task due to the inherent instability of hydrogen peroxide molecules. Consequently, the development and use of computational tools have become essential for exploring the stability and key processes of these species, such as ionization. These approaches can help address existing gaps in scientific understanding and aid in the future identification and characterization of various conformations of the H_2O_2 aggregates. To date, there are no available data in the literature regarding the existence or stability of potential conformations of H_2O_2 dimers. This lack of information, combined with the pioneering experimental efforts by Pysanenko et al.,[38] served as the main motivation for conducting this current study.

In this work, we elaborated and performed a systematic investigation of the structures, energetics, and ionization energies (IEs) of a series of hydrogen peroxide clusters, more specifically, the dimers $(H_2O_2)_2$. While stable conformations typically dominate biological interactions, high-energy forms can transiently contribute when flexibility allows necessary structural adaptations. Hence, a combination of conformational analysis and high-levels of theory, i.e., coupled-cluster, approaches was employed for exploring the forms of existence, relative stabilities, and ionization processes of a series of conformations of $(H_2O_2)_2$. At the end, important insights were gathered regarding both the physical-chemical perspective and, secondarily, the possibility of using sequentially combined theoretical methodologies. We hope that this work may serve as motivation for computational and experimental studies of larger $(H_2O_2)_2$ clusters for study in the near future.

■ COMPUTATIONAL METHODS

Structures and Energetics. First, the conformer-rotamer ensemble sampling tool (CREST)[39] was used to identify low-lying conformers of the H_2O_2 dimers at the GFN2-xTB[40] level of theory in the gas phase. These were subsequently fully optimized using the B3LYP exchange−correlation functional[41,42] with the 6−311+G(d,p) basis set,[43−46] also in the gas phase. The Boltzmann distribution of these conformers was determined through the use of GoodVibes[47] software. The geometry of each stable conformer found at the B3LYP/6−311+G(d,p) level of theory was then reoptimized using the coupled-cluster with single, double, and perturbative triple excitations (CCSD(T)) approach[48,49] with the aug-cc-pVTZ[50,51] basis sets (from this moment on referred to as AVTZ) in the gas phase. Harmonic vibrational frequencies were determined at this same level to characterize each structure as a minima on the potential energy surface and for evaluating zero-point vibrational corrections to the electronic energies. The density functional theory computations were accomplished with the Gaussian 09[52] package, while the latest version of the MOLPRO[53] suite of software was used for performing all of the CCSD(T) calculations.

Ionization Energies. The lowest-lying vertical IEs of all of the conformations of the H_2O_2 dimer were computed through the use of the equation-of-motion ionization potential coupled-cluster with single and double excitations approach (EOMIP-CCSD)[54] with the aug-cc-pVnZ basis sets (n = D, T, Q) at the CCSD(T)/AVTZ structures as obtained for each conformer. To explore the contributions of core−valence correlation (Δ_{CV}), two EOMIP-CCSD calculations were carried out with the aug-cc-pCVnZ (n = D, T) basis sets (that will be denoted by ACVnZ hereafter). The first of the computations was performed considering all of the electrons correlated, while the second was accomplished through correlating only the valence electrons. Thus, the Δ_{CV} contribution was obtained by the difference between the corresponding results from these two computations. The EOMIP-CCSD total energies were extrapolated to the complete basis set (CBS) limits with the equation proposed by Martin[55] as

$$E_n = E_{CBS} + A(n + 1/2)^{-4} \tag{1}$$

where E are the total energies and n is the cardinal number associated with a given basis set (for instance, n = 3 in the AVTZ).

The composite IEs were determined with an adapted version[56−58] of the Feller−Peterson−Dixon (FPD) composite approach[59] as

$$IE_{FPD} = IE_{AVTZ} + \Delta_{CBS} + \Delta_{CV} \tag{2}$$

where the Δ_{CBS} component is obtained as the difference between a given ionization energy computed at the EOMIP-CCSD/AVTZ level and its respective value estimated at the

CBS limit. All of the EOMIP-CCSD computations were performed using the CFOUR[60] package.

The sequentially combined theoretical approaches regarding the selection of the relevant conformations and the exploration of the corresponding ionization processes for molecular clusters were proposed, with their summarized scheme being shown in Figure 1.
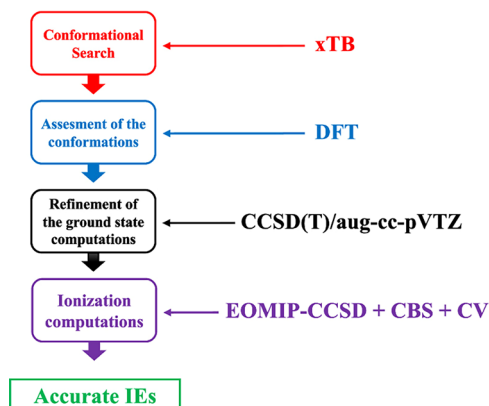

Figure 1. Illustration of the sequentially combined theoretical approaches employed in this work.

RESULTS AND DISCUSSION

Initially, a total of 13 possible rotamers of the H_2O_2 dimer were suggested to exist at the GFN2-xTB[40] level of theory (in the gas phase). Subsequently, each cluster was reoptimized using the B3LYP exchange−correlation functional with the 6−311+G(d,p) basis set; respective harmonic vibrational frequencies were computed at B3LYP/6−311+G(d,p). After the evaluation of the vibrational frequencies of the (13) initial rotamers, seven were identified as not being minima on the corresponding potential energy surfaces. The six stable conformations of the H_2O_2 dimer at the B3LYP/6−311+G-(d,p) level of theory were found to have Boltzmann distributions larger than 1%. The chemical structures of the six H_2O_2 conformers are shown in Figure 2. Conformations I
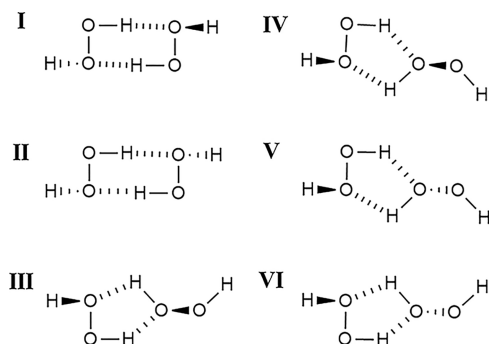

Figure 2. Illustration of the chemical structures of the H_2O_2 dimers.

and II of the H_2O_2 dimer presented Boltzmann distributions of 47.50 and 30.80%, respectively, which are considerably higher than those determined for the other conformations. Conformations III and IV exhibited very close values (6.10% versus 6.20%), while conformations V and VI were found to present identical results (4.80%) for the Boltzmann distributions.

The six structures of the H_2O_2 dimer presented in Figure 2 were used as initial guesses for optimizations at the CCSD(T)/AVTZ level of theory. The final CCSD(T)/AVTZ fully optimized structures with their corresponding bond distances and interactions are shown in Figure 3. In general, each system investigated presented two hydrogen bonds in its chemical structure, with conformations I and II presenting the strongest ones, as can be inferred from the O···H distances (from 1.905 to 1.907 Å). These intermolecular distances are comparable to (although slightly smaller than) the 1.9485 Å obtained by Tschumper et al.[61] for the nonplanar open Cs conformation of the water dimer at the CCSD(T)/TZ2P(f,d)+diffuse level of theory, suggesting that the hydrogen-bonding interactions are marginally stronger in the H_2O_2 dimer in comparison to the H_2O dimer. Overall, the intramolecular distances obtained for any of the conformations of the H_2O_2 dimer are comparable to the corresponding distances reported in the literature for dimers of similar molecules, such as water, ethylene glycol, and ethanol.[61−69] Taking the conformation I (the strongest conformer) as instance, the length of the O−H bonds undergoing hydrogen interaction was determined to be 0.975 Å at the CCSD(T)/AVTZ level of theory, which is only slightly enlarged when compared to the 0.972 and 0.965 Å reported in the case of the nonplanar open Cs conformation of the water dimer by Miliordos and Xantheas[70] at the CCSD(T)/AVDZ level and by Tschumper et al.[61] at the CCSD(T)/TZ2P(f,d)+diffuse level, respectively. Interestingly, the structure obtained for conformation IV was found to be a mirror image when compared to that of conformation III; the same behavior was noticed in the case of conformations V and VI. These observations may be an indication that these two pairs of H_2O_2 dimers may represent only two actual chemical species. Cartesian coordinates of all of the optimized structures are available in the Supporting Information.

The relative energies (ΔE_{conf}) and binding energies (ΔE_b) determined with the CCSD(T) approach for the conformations of the H_2O_2 dimers can be found in Table 1. Conformation I was found to be the strongest bound, presenting a binding energy of −37.2 kJ/mol at the CCSD(T)/CBS[TQ] level that decreased in magnitude to −27.4 kJ/mol at 0 K when the zero-point corrections to the electronic energies were included. The weakest bound species are the conformations V and VI with binding energies of −19.9 kJ/mol at 0K; these conformations presented exactly the same results for their energetic properties, and thus, the mirror images represent (for practical purposes) the same chemical entity. The same behavior was observed for conformations V and VI, which (along with conformations III and IV) will be grouped together and referred to as a single system from this point on. This definition is certainly an important part of the methodology, as it can yield a considerable degree of economy in terms of computational effort. The averaged binding energies obtained with CCSD(T)/AVTZ were determined to be different by (approximately) 5% in comparison to the CCSD(T)/CBS[TQ] results, which suggests the use of the triple-ζ basis set as being an adequate choice to be used in these type of systems, particularly when considering the investigation of molecular clusters containing a large number of H_2O_2 molecules. All of the conformations of the H_2O_2 dimer presented binding energies that suggested these species as being more strongly bound than the H_2O dimers. For instance, Miliordos and Xantheas[63] estimated the ΔE_b of the
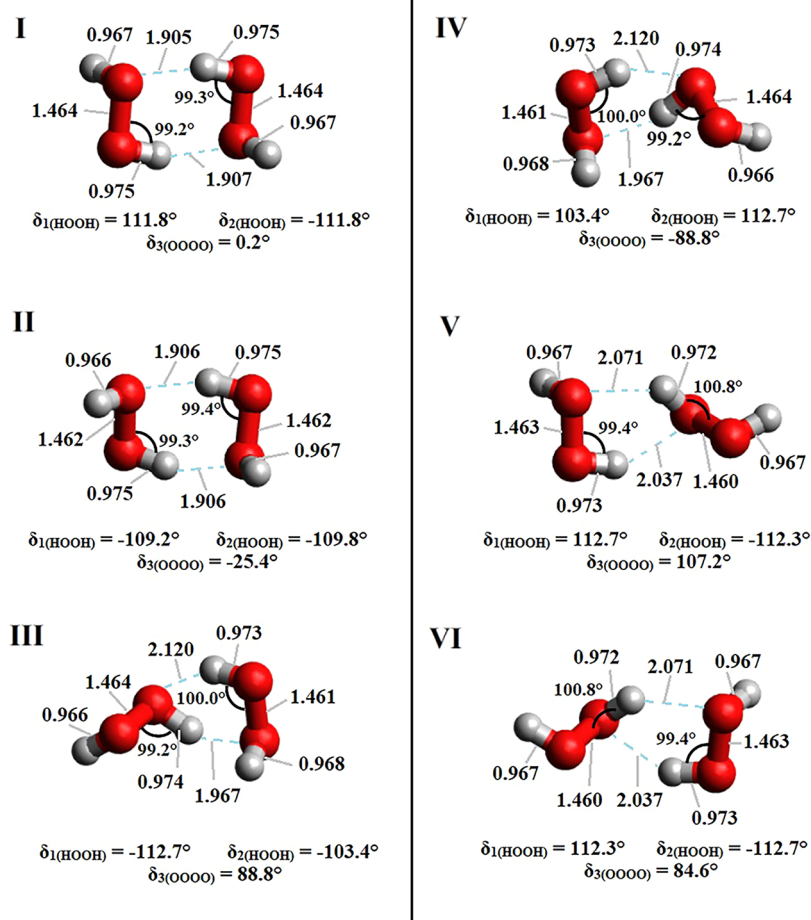
Figure 3. Ground-state structures of six conformations of the H_2O_2 dimer optimized at the CCSD(T)/AVTZ level of theory. Inter and intramolecular bond distances are given in Å.

Table 1. Relative Energies (ΔE_{conf}) and Binding Energies (ΔE_b) of the Conformations of the H_2O_2 Dimers, as Obtained at the CCSD(T) Level[a]

conformation	AVTZ	CBS	ΔZPE	$\Delta E_b^{CBS}(0K)$	$\Delta E_{conf}^{CBS}(0K)$
I	−39.37	−37.20	9.79	−27.41	0.00
II	−38.46	−36.48	9.71	−26.77	0.72
III and IV	−31.40	−29.70	8.00	−21.70	7.50
V and VI	−29.11	−27.58	7.69	−19.89	9.62

[a]The values are given in kJ/mol.

H_2O dimer as −4.99 ± 0.04 kcal/mol at the CCSD(T)/CBS level.

As the chemical species under investigation in the present work consist of only hydrogen and oxygen atoms, it is expected that scalar relativity effects would play negligible roles in all their energetic properties. To verify this assumption, the binding energies of each conformation of the H_2O_2 dimers obtained at the CCSD(T)/AVTZ level were compared to corresponding results determined using the aug-cc-pVTZ-DK basis sets[71] with the second-order Douglas-Kroll-Hess scalar relativistic Hamiltonian.[72,73] At the end, the biggest relativistic contribution was determined to be just 0.09 kJ/mol in the case of conformation II, which is consistent with the finding reported in very recent work involving $H_2CO\cdots HNO$ species.[74] Hence, taking such effects into consideration is not necessary for these actual systems and is not advised for larger clusters composed of H_2O_2, as the additional computations

may represent a considerable increase in the computational cost (if computed as an additive contribution).

The tables containing the ten lowest-lying vertical IEs of each conformation of the H_2O_2 dimers, as determined using the EOMIP-CCSD approach with the AVDZ, AVTZ, and AVQZ basis sets, can be found in the Supporting Material (SM). The number of the IEs that were explored originated from the ideas prescribed by Tanaka et al.[75] when studying the photoionization of the formaldehyde molecule. The authors concluded that a reasonable number of inner orbitals would be necessary for accurately obtaining various fundamental quantities, such as the photoionization cross sections.[75] Hence, providing a considerably large amount of IEs may be useful as auxiliary (and input data) for other research to be based upon in the future. The IEs determined using the EOMIP-CCSD methods at the CBS limit are also available in the SM. Overall, all of the results determined for any conformation of the H_2O_2 dimer indicated an increase in the IEs with an increase in the size of the aug-cc-pVnZ basis set used. Taking conformation I, for example, the first IE was computed to be 11.31 eV at EOMIP-CCSD/AVDZ, 11.54 eV at EOMIP-CCSD/AVTZ, and 11.63 eV at EOMIP-CCSD/AVQZ. The CBS[DT] IEs were found to be in considerably better agreement than CBS[TQ] when compared with the corresponding results obtained with the AVQZ basis set. However, although this observation may be tempting for the researcher in regards of choosing CBS[DT] over the

CBS[TQ] extrapolation, especially for large clusters containing the H_2O_2 molecule, the option for the CBS[TQ] is certainly advised in every case where the quadruple-ζ computations were feasible.

The composite IEs and their individual contributions are shown in Table 2. The first IE of conformation V was determined to be 11.58 eV, which is the lowest among all of the IEs for the other conformations of the H_2O_2 dimer,

Table 2. Composite EOMIP-CCSD Vertical IEs (in eVs) of the H_2O_2 Dimers

conformation	I	II	III = IV	V = VI
		IE 1		
E_{AVTZ}	11.54	11.50	11.65	11.41
$\Delta_{CBS[TQ]}$	0.15	0.14	0.15	0.14
Δ_{CV}	0.03	0.03	0.03	0.03
IP_{FPD}	11.72	11.67	11.83	11.58
		IE 2		
E_{AVTZ}	11.61	11.75	11.74	11.69
$\Delta_{CBS[TQ]}$	0.15	0.14	0.14	0.14
Δ_{CV}	0.03	0.03	0.03	0.03
IP_{FPD}	11.79	11.92	11.91	11.86
		IE 3		
E_{AVTZ}	12.27	12.30	12.44	12.56
$\Delta_{CBS[TQ]}$	0.14	0.14	0.14	0.14
Δ_{CV}	0.03	0.03	0.03	0.03
IP_{FPD}	12.44	12.47	12.61	12.73
		IE 4		
E_{AVTZ}	13.37	13.10	12.71	12.71
$\Delta_{CBS[TQ]}$	0.14	0.14	0.14	0.14
Δ_{CV}	0.03	0.03	0.03	0.03
IP_{FPD}	13.54	13.27	12.88	12.88
		IE 5		
E_{AVTZ}	15.48	15.47	15.42	15.22
$\Delta_{CBS[TQ]}$	0.12	0.13	0.12	0.13
Δ_{CV}	0.02	0.02	0.02	0.03
IP_{FPD}	15.62	15.62	15.56	15.38
		IE 6		
E_{AVTZ}	15.51	15.60	15.62	15.64
$\Delta_{CBS[TQ]}$	0.12	0.12	0.12	0.12
Δ_{CV}	0.03	0.03	0.02	0.02
IP_{FPD}	15.66	15.75	15.76	15.78
		IE 7		
E_{AVTZ}	16.74	16.60	16.95	17.06
$\Delta_{CBS[TQ]}$	0.13	0.13	0.13	0.12
Δ_{CV}	0.02	0.02	0.02	0.02
IP_{FPD}	16.89	16.75	17.10	17.20
		IE 8		
E_{AVTZ}	18.19	18.26	17.90	17.81
$\Delta_{CBS[TQ]}$	0.12	0.12	0.12	0.11
Δ_{CV}	0.02	0.02	0.02	0.02
IP_{FPD}	18.33	18.40	18.04	17.94
		IE 9		
E_{AVTZ}	18.64	18.70	18.61	18.43
$\Delta_{CBS[TQ]}$	0.11	0.11	0.11	0.11
Δ_{CV}	0.02	0.02	0.02	0.02
IP_{FPD}	18.77	18.83	18.74	18.56
		IE 10		
E_{AVTZ}	18.74	18.72	18.73	18.75
$\Delta_{CBS[TQ]}$	0.11	0.11	0.11	0.10
Δ_{CV}	0.02	0.02	0.02	0.02
IP_{FPD}	18.87	18.85	18.86	18.87

followed by the results obtained for conformations II (11.67 eV), I (11.72 eV), and III (11.83 eV). In principle, the differences observed may be helpful for the assignments in future experiments. On the other hand, it is relevant to notice that the second IEs of conformations I and V were computed to be considerably close to the first IE of conformation III of $(H_2O_2)_2$; more precisely, these results were determined to be −0.04 eV and +0.03 eV in comparison to 11.83 eV, respectively. This situation may bring eventual difficulties to the assignment process, given that the differences in the referred IEs are within chemical accuracy, and thus, it will demand not only the use of techniques with high spectroscopic resolution but also a careful analysis of the results measured. The core-correlation effects were found to be considerably small (with the largest contributions to the IEs being +0.03 eV), as can be noticed from the Δ_{CV} results that are also shown in Table 2. All of the raw energy values that are required for composing the final IEs are also available in the Supporting Information. In terms of the contribution of each molecular fragment to the ionization of the dimers, it is possible to notice from the highest occupied molecular orbital (HOMO) to the HOMO −6 plots (also available in the Supporting Information) that the ionization processes have a delocalized nature in all of the conformations of the $(H_2O_2)_2$.

The composite (vertical) IEs and their individual contributions for the H_2O_2 monomer are shown in Table 3. Overall,

Table 3. Composite EOMIP-CCSD Vertical IEs (in eVs) of the H_2O_2 Molecule

IE	E_{AVTZ}	$\Delta_{CBS[TQ]}$	Δ_{CV}	IP_{FPD}
1	11.54	0.14	0.03	11.71
2	12.58	0.13	0.03	12.74
3	15.38	0.13	0.02	15.53
4	17.40	0.12	0.02	17.54
5	18.55	0.10	0.02	18.67
6	21.37	0.31	0.15	21.83
7	23.02	0.31	0.15	23.48
8	23.78	0.29	0.15	24.22
9	24.28	0.29	0.14	24.71
10	26.32	0.29	0.14	26.75

the $\Delta_{CBS[TQ]}$ and Δ_{CV} contributions to the five lowest-lying IEs of the H_2O_2 molecule were found to be comparable to those obtained for all of the IEs of the dimers. However, a pronounced increase in these contributions was noticed in the case of the high-lying IEs. The first composite vertical ionization energy of H_2O_2 was computed to be 11.71 eV, a value that is approximately 1 eV larger than the 10.638 ± 0.012 eV *adiabatic* ionization energy as obtained by Changala et al.[76] with an approach based on high-level computations, a difference that is due primarily to the changes in the molecular structure after the ionization, with the ionized geometry presenting a dihedral of 180.0° (see Figure 4). In the current work, the CCSD(T)/AVTZ vertical and equilibrium IEs are 11.67 and 10.57 eV, respectively. Interestingly, the first vertical IE of the H_2O_2 monomer was determined to be very close to the corresponding result obtained for conformation I of the H_2O_2 dimer. Actually, the molecular system presented the vertical IE_1 as being only 0.01 eV lower than the respective ionization energy of conformation I of the H_2O_2 dimer. This observation could suggest that knowing only the IEs of the isolated molecule might (perhaps) suffice for describing the
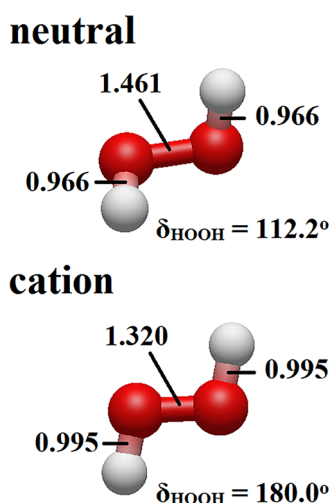
Figure 4. Structures of the neutral and cationic forms of the H_2O_2 monomer, as optimized at the CCSD(T)/AVTZ level of theory. Inter- and intramolecular bond distances are given in Å.

Figure 5. Structures of the cationic forms of the H_2O_2 dimer as optimized at the CCSD(T)/aVTZ level of theory. Inter- and intramolecular bond distances are given in Å.

ionization processes of the most stable conformation of the H_2O_2 dimer, which can actually be misleading, as the behavior vanishes when comparing the other IEs, with the differences between the results determined for the monomer and dimers continuing to grow especially for the high-lying IEs. In terms of comparison with results obtained experimentally for a similar system, the first and second IEs obtained for any conformation of the H_2O_2 dimer are slightly lower in comparison to the experimental results reported for the water dimer by Tomoda et al.[77] through the use of a nozzle beam photoelectron spectrometer; the authors obtained these IEs as being 12.1 ± 0.1 eV and 13.2 ± 0.2 eV, respectively.

In a manner similar to that observed in the comparison of the vertical and the adiabatic IEs obtained for the H_2O_2 monomer, the latter determined for the H_2O_2 dimers were also found to be considerably lower than the corresponding vertical IEs. In particular, the first equilibrium IEs for dimers I, II, III—IV, and V—VI are (in eV) 9.52, 9.51, 9.44, and 9.41, respectively, as calculated at the CCSD(T)/AVTZ level of theory. The corresponding CCSD(T)/AVTZ values for the vertical IE are 11.70, 11.70, 11.78, and 11.56 eV, respectively. Interestingly, the order of these IEs is also slightly different from that noticed when not considering the reorganization of the molecular geometry after the ionization. In comparison to the EOMIP-CCSD vertical IEs of Table 2, the CCSD(T) values are about 0.15 to 0.20 eV larger. This is only slightly larger than the difference between EOMIP-CCSD and CCSD(T) for the monomer. Pronounced changes in the chemical structures of the cations of the H_2O_2 dimers were also seen, with each of the two monomers being strongly bonded by the plane-oriented O···H···O interaction. The structures of the cationic forms of the H_2O_2 dimer, as optimized at the R/UCCSD(T)/aVTZ level of theory (restricted open-shell Hartree—Fock orbitals with unrestricted CCSD as implemented in Molpro[78]), can be found in Figure 5. The large structural changes upon ionization lead to differences between the vertical and equilibrium IEs of about a factor of 2 larger than what is calculated for the monomer, i.e., about −2.2 eV in the dimers compared to −1.0 eV in the monomer.
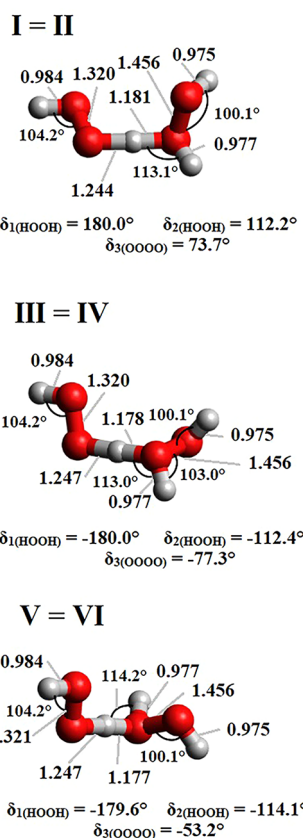
CONCLUSIONS

We performed an investigation of the ground-state binding energies and ionization processes of a series of hydrogen peroxide clusters. The most stable aggregation form of the H_2O_2 dimer was found to be conformation I, which was determined as being only 0.72 kJ/mol lower than conformation II at the CCSD(T)/CBS level of theory; the other stable conformations were calculated to be within 10 kJ/mol from conformation I at the same CCSD(T)/CBS level of theory. The differences observed in the IEs of $(H_2O_2)_2$ can be important for the assignments of experimental data regarding the identification of the different conformations of such clusters. Given that the H_2O_2 clusters were first isolated through beam experiments in recent years, it is expected that the present work might call the attention of the scientific community to this system, and these results will hopefully motivate future experimental and theoretical investigations. More specifically, investigations targeting the exploration of how the different H_2O_2 dimer conformers would behave when interacting with macromolecular, biological, and food systems would certainly be welcome.

ASSOCIATED CONTENT

ⓢ Supporting Information

The Supporting Information is available free of charge at https://pubs.acs.org/doi/10.1021/acs.jctc.5c01330.

Individual energy contributions to the vertical ionization energies for all of the conformations of the H_2O_2 dimer, raw electronic energy values, Cartesian coordinates of

the optimized structures, and molecular orbital plots (PDF)

AUTHOR INFORMATION

Corresponding Authors

Kirk A. Peterson − *Department of Chemistry, Washington State University, Pullman, Washington 99164, United States;* ● orcid.org/0000-0003-4901-3235; Email: kipeters@wsu.edu

Gabriel L. C. de Souza − *Centro de Cîencias da Natureza, Universidade Federal de São Carlos, Buri, São Paulo 18290-000, Brazil;* ● orcid.org/0000-0002-2192-7345; Phone: +1-509-335-7867; Email: gabriellcs@ufscar.br

Author

José L. F. Santos − *Instituto de Química de São Carlos, Universidade São Paulo, São Carlos, São Paulo 13566-590, Brazil;* ● orcid.org/0000-0003-1562-5233

Complete contact information is available at:
https://pubs.acs.org/10.1021/acs.jctc.5c01330

Notes

The authors declare no competing financial interest.

ACKNOWLEDGMENTS

REFERENCES

(1) Sirotkin, V. A. Lysozyme in Mixtures of Hydrogen Bond Acceptor Solvents with Water: Enthalpies and Entropies of Preferential Solvation. *J. Phys. Chem. B* **2025**, *129*, 5386−5399.

(2) Castillo-Orellana, C.; Heidar-Zadeh, F.; Vöhringer-Martinez, E. Nonbonded Force Field Parameters Derived from Atoms-in-Molecules Methods Reproduce Interactions in Proteins from First-Principles. *J. Chem. Theory Comp.* **2025**, *21*, 2043−2054.

(3) Ahmad, K.; Ahmad, R.; Nadia, B.; Khan, S.; Khan, M. J.; Yasin, M. T.; Khan, T. U.; Ahmed, I. Marine collagen bio-composites materials: Interactions with small active molecules and their application in food industry. *Int. J. Biol. Macromol.* **2025**, *307*, No. 142237.

(4) Xie, S. Y.; Karnaukh, K. M.; Yang, K. C.; Sun, D.; Delaney, K. T.; de Alaniz, J. R.; Fredrickson, G. H.; Segalman, R. A. Compatibilization of Polymer Blends by Ionic Bonding. *Macromolecules* **2023**, *56*, 3617−3630.

(5) Minecka, A.; Tarnacka, M.; Jurkiewicz, K.; Hachula, B.; Wrzalik, R.; Kaminski, K.; Paluch, M.; Kaminska, E. Impact of the Chain Length and Topology of the Acetylated Oligosaccharide on the Crystallization Tendency of Naproxen from Amorphous Binary Mixtures. *Mol. Pharmaceutics* **2021**, *18*, 347−358.

(6) Ura, T.; Arakawa, T.; Shiraki, K. Insight into the protein salting-in mechanism of arginine, magnesium chloride and ethylene glycol: Solvent interaction with aromatic solutes. *Int. J. Biol. Macromol.* **2021**, *188*, 670−677.

(7) Özbagcr, D. I.; Erdagr, S. I.; Aydin, R. Evaluation of the interaction of food dye fast green FCF with the digestive enzyme trypsin. *J. Mol. Struct.* **2025**, *1338*, No. 142344.

(8) Lal, K.; Grover, A.; Ragshaniya, A.; Aslam, M.; Singh, P.; Kumari, K. Current advancements and future perspectives of 1,2,3-triazoles to target lanosterol 14-α-demethylase (CYP51), a cytochrome P450 enzyme: A computational approach. *Int. J. Biol. Macromol.* **2025**, *315*, No. 144240.

(9) Ishak, S. N. H.; Saad, A. H. M.; Latip, W.; Rahman, R. N. Z. R. A.; Salleh, A.; Kamarudin, N. H. A.; Leow, A. T. C.; Ali, M. S. M. Enhancing industrial biocatalyst performance and cost-efficiency through adsorption-based enzyme immobilization: A review. *Int. J. Biol. Macromol.* **2025**, *316*, No. 144278.

(10) Santos, J. L. F.; de Souza, G. L. C. Water hydrogen-bonding effects on the ground and low-lying excited states of dipyridyl isomers. *J. Mol. Liq.* **2021**, *338*, No. 116767.

(11) Santos, J. L. F.; de Souza, G. L. C. Insights into the photoinduced degradation of terbuthylazine from aqueous solution: The synergic effects generated from hydrogen-bond interactions. *J. Mol. Liq.* **2022**, *358*, No. 119139.

(12) Filho, A. H. d. S.; Candeias, F. S.; da Silva, S. C.; Vicentini, F. C.; Assumpção, M. H. M. T.; Brown, A.; de Souza, G. L. C. Photoinduced degradation of indigo carmine: insights from a computational investigation. *J. Mol. Model.* **2020**, *26*, No. 309.

(13) da Mata, V. A. S.; Mendes, R. A.; de Souza, G. L. C. Impact of conformation on electron-scattering cross sections for formaldehyde dimers. *Phys. Rev. A* **2018**, *98*, No. 042707.

(14) Mendes, R. A.; da Mata, V. A. S.; Brown, A.; de Souza, G. L. C. A density functional theory benchmark on antioxidant-related properties of polyphenols. *Phys. Chem. Chem. Phys.* **2024**, *26*, 8613.

(15) Soares, I. N.; Peterson, K. A.; de Souza, G. L. C. Probing Antioxidant-Related Properties for Phenolic Compounds. *J. Phys. Chem. A* **2024**, *128*, 2727−2736.

(16) Greenwood, N. N.; Earnshaw, A. Chemistry of the Elements - 2nd Edition, 1997.

(17) Sies, H. Role of Metabolic H_2O_2 Generation. *J. Biol. Chem.* **2014**, *289*, 8735−8741.

(18) Yukl, E. T.; Williamson, H. R.; Higgins, L.; Davidson, V. L.; Wilmot, C. L. Oxidative Damage in MauG: Implications for the Control of High-Valent Iron Species and Radical Propagation Pathways. *Biochem* **2013**, *52*, 9447−9455.

(19) Lennicke, C.; Rahn, J.; Lichtenfels, R.; Wessjohann, L. A.; Seliger, B. Hydrogen peroxide - production, fate and role in redox signaling of tumor cells. *Cell Commun. Signal* **2015**, *13*, No. 39.

(20) Slauch, J. M. How does the oxidative burst of macrophages kill bacteria? Still an open question. *Mol. Microbiol.* **2011**, *80*, 580−583.

(21) Saputra, F.; Kishida, M.; Hu, S.-Y. Oxidative stress induced by hydrogen peroxide disrupts zebrafish visual development by altering apoptosis, antioxidant and estrogen related genes. *Sci. Rep.* **2024**, *14*, No. 14454.

(22) Chopra, N.; Kaur, D.; Chopra, G. Nature and Hierarchy of Hydrogen-Bonding Interactions in Binary Complexes of Azoles with Water and Hydrogen Peroxide. *ACS Omega* **2018**, *3*, 12688−12702.

(23) Grzechnik, K.; Mierzwicki, K.; Mielke, Z. Matrix-Isolated Hydrogen-Bonded and Van der Waals Complexes of Hydrogen Peroxide with OCS and CS_2 ChemPhysChem. *ChemPhysChem* **2013**, *14*, 777−787.

(24) Mucha, M.; Mielke, Z. Photochemistry of the glyoxal-hydrogen peroxide complexes in solid argon: Formation of 2-hydroxy-2-hydroperoxyethanal. *Chem. Phys. Lett.* **2009**, *482*, 87−92.

(25) Engdahl, A.; Nelander, B. The HOOH-HOO complex. A matrix isolation study. *Phys. Chem. Chem. Phys.* **2004**, *6*, 730−734.

(26) Goebel, J. R.; Antle, K. A.; Ault, B. S.; Del Bene, J. E. Matrix Isolation and ab Initio Study of 1:1 Hydrogen-Bonded Complexes of H_2O_2 with HF, HCl, and HBr. *J. Phys. Chem. A* **2002**, *106*, 6406−6414.

(27) Lundell, J.; Jolkkonen, S.; Khriachtchev, L.; Pettersson, M.; Räsänen, M. Matrix Isolation and Ab Initio Study of the Hydrogen-Bonded H_2O_2 − CO Complex. *Chemistry* **2001**, *7*, 1670−1678.

(28) Lundell, J.; Pehkonen, S.; Petterson, M.; Räsänen, M. Interaction between hydrogen peroxide and molecular nitrogen. *Chem. Phys. Lett.* **1998**, *286*, 382−388.

(29) da Silva, L. M.; Mena, I. F.; Saex, C.; Motheo, A. J.; Rodrigo, M. A. Treatment of Organics in Wastewater Using Electrogenerated Gaseous Oxidants. *Ind. Eng. Chem. Res.* **2024**, *63*, 6512−6520.

(30) Kremer, M. L. Initial Steps in the Reaction of H2O2 with Fe$^{2.}$ and Fe$^{3.}$ Ions: Inconsistency in the Free Radical Theory. *Reactions* **2023**, *4*, 171−175.

(31) King, D. W.; Farlow, R. Role of carbonate speciation on the oxidation of Fe(II) by H$_2$O$_2$. *Mar. Chem.* **2000**, *70*, 201−209.

(32) Priyadarsini, A.; Mallik, B. S. Structure and rotational dynamics of water around hydrogen peroxide. *J. Mol. Liq.* **2022**, *348*, No. 118054.

(33) Biswas, A.; Mallik, B. S. Conformation-induced vibrational spectral dynamics of hydrogen peroxide and vicinal water molecules. *Phys. Chem. Chem. Phys.* **2021**, *23*, 6665−6676.

(34) Biswas, A.; Mallik, B. S. Conformational dynamics of aqueous hydrogen peroxide from first principles molecular dynamics simulations. *Phys. Chem. Chem. Phys.* **2020**, *22*, 28286−28296.

(35) Medvedev, A. G.; Egorov, P. A.; Mikhaylov, A. A.; Belyaev, E. S.; Kirakosyan, G. A.; Gorbunova, Y. G.; Filippov, O. A.; Belkova, N. V.; Shubina, E. S.; Brekhovskikh, M. N.; Kirsanova, A. A.; Babak, M. V.; Lev, O.; Prikhodchenko, P. V. Synergism of primary and secondary interactions in a crystalline hydrogen peroxide complex with tin. *Nat. Commun.* **2024**, *15*, No. 5758.

(36) Joshipura, K. N.; Pandya, S. H.; Mason, N. J. Electron scattering and ionization of H$_2$O; OH, H$_2$O$_2$, HO$_2$ radicals and (H$_2$O)$_2$ dimer. *Eur. Phys. J. D* **2017**, *71*, No. 96.

(37) Nandi, D.; Krishnakumar, E.; Rosa, A.; Schmidt, W.-F.; Illenberger, E. Dissociative electron attachment to H2O2: a very effective source for OH and OH$^−$ generation. *Chem. Phys. Lett.* **2003**, *373*, 454−459.

(38) Pysanenko, A.; Pluharová, E.; Vinklárek, I. S.; Rakovský, J.; Poterya, V.; Kočišek, J.; Fárník, M. Ion and radical chemistry in (H$_2$O$_2$)$_N$ clusters. *Phys. Chem. Chem. Phys.* **2020**, *22*, No. 15312.

(39) Pracht, P.; Bohle, F.; Grimme, S. Automated exploration of the low-energy chemical space with fast quantum chemical methods. *Phys. Chem. Chem. Phys.* **2020**, *22*, 7169−7192.

(40) Grimme, S. Exploration of chemical compound, conformer, and reaction space with meta-dynamics simulations based on tight-binding quantum chemical calculations. *J. Chem. Theory Comp.* **2019**, *15*, 2847−2862.

(41) Becke, A. D., III Density-Functional Thermochemistry. III. The Role of Exact Exchange. *J. Chem. Phys.* **1993**, *98*, 5648−5652.

(42) Lee, C.; Yang, W.; Parr, R. G. Development of the Colle-Salvetti Correlation-Energy Formula into a Functional of the Electron Density. *Phys. Rev. B* **1988**, *37*, No. 785.

(43) Rassolov, V. A.; Pople, J. A.; Ratner, M.; Redfern, P. C.; Curtiss, L. A. 6−31G*Basis Set for Third-Row Atoms. *J. Comput. Chem.* **2001**, *22*, 976−984.

(44) Binkley, J. S.; Pople, J. A.; Hehre, W. J. Self-Consistent Molecular Orbital Methods. 21. Small Split-Valence Basis Sets for First-Row Elements. *J. Am. Chem. Soc.* **1980**, *102*, 939−947.

(45) Frisch, M. J.; Pople, J. A.; Binkley, J. S. Self-Consistent Molecular Orbital Methods 25. Supplementary Functions for Gaussian Basis Sets. *J. Chem. Phys.* **1984**, *80*, 3265−3269.

(46) Hehre, W. J.; Ditchfield, R.; Pople, J. A. Self-Consistent Molecular Orbital Methods. XII. Further Extensions of Gaussian Type Basis Sets for Use in Molecular Orbital Studies of Organic Molecules. *J. Chem. Phys.* **1972**, *56*, 2257−2261.

(47) Luchini, G.; Alegre-Requena, J. V.; Funez-Ardoiz, I.; Paton, R. S. GoodVibes: automated thermochemistry for heterogeneous computational chemistry data. *F1000Research* **2020**, *9*, No. 291.

(48) Raghavachari, K.; Trucks, G. W.; J A Pople, J. A.; Head-Gordon, M. A fifth-order perturbation comparison of electron correlation theories. *Chem. Phys. Lett.* **1989**, *157*, 479−483.

(49) Bartlett, R. J.; Watts, J. D.; Kucharski, S. A.; Noga, J. Non-iterative fifth-order triple and quadruple excitation energy corrections in correlated methods. *Chem. Phys. Lett.* **1990**, *165*, 513−522.

(50) Dunning, T. H. Gaussian basis sets for use in correlated molecular calculations. *J. Chem. Phys.* **1989**, *90*, 1007−1023.

(51) Kendall, R. A.; Dunning, T. H.; Harrison, R. J. Electron affinities of the first-row atoms revisited. Systematic basis sets and wave functions. *J. Chem. Phys.* **1992**, *96*, 6796−6806.

(52) Frisch, M. J.; Trucks, G. W.; Schlegel, H. B.; Scuseria, G. E.; Robb, M. A.; Cheeseman, J. R.; Scalmani, G.; Barone, V.; Mennucci, B.; Petersson, G. A.; Nakatsuji, H.; Caricato, M.; Li, X.; Hratchian, H. P.; Izmaylov, A. F.; Bloino, J.; Zheng, G.; Sonnenberg, J. L.; Hada, M.; Ehara, M.; Toyota, K.; Fukuda, R.; Hasegawa, J.; Ishida, M.; Nakajima, T.; Honda, Y.; Kitao, O.; Nakai, H.; Vreven, T.; Montgomery, J. A., Jr.; Peralta, J. E.; Ogliaro, F.; Bearpark, M.; Heyd, J. J.; Brothers, E.; Kudin, K. N.; Staroverov, V. N.; Kobayashi, R.; Normand, J.; Raghavachari, K.; Rendell, A.; Burant, J. C.; Iyengar, S. S.; Tomasi, J.; Cossi, M.; Rega, N.; Millam, N. J.; Klene, M.; Knox, J. E.; Cross, J. B.; Bakken, V.; Adamo, C.; Jaramillo, J.; Gomperts, R.; Stratmann, R. E.; Yazyev, O.; Austin, A. J.; Cammi, R.; Pomelli, C.; Ochterski, J. W.; Martin, R. L.; Morokuma, K.; Zakrzewski, V. G.; Voth, G. A.; Salvador, P.; Dannenberg, J. J.; Dapprich, S.; Daniels, A. D.; Farkas, O.; Foresman, J. B.; Ortiz, J. V.; Cioslowski, J.; Fox, D. J. *Gaussian 09, Revision D.01*.; Gaussian, Inc.: Wallingford CT, 2009.

(53) Werner, H.-J.; Knowles, P. J.; Manby, F. R.; Black, J. A.; Doll, K.; Hesselmann, A.; Kats, D.; Köhn, A.; Korona, T.; Kreplin, D. A.; Ma, Q.; Miller, T. F.; Mitrushchenkov, A.; Peterson, K. A.; Polyak, I.; Rauhut, G.; Sibaev, M. The Molpro quantum chemistry package. *J. Chem. Phys.* **2020**, *152*, No. 144107.

(54) Stanton, J. F.; Bartlett, R. J. The equation of motion coupled-cluster method. A systematic biorthogonal approach to molecular excitation energies, transition probabilities, and excited state properties. *J. Chem. Phys.* **1993**, *98*, 7029−7039.

(55) Martin, J. M. L. Ab initio total atomization energies of small molecules - towards the basis set limit. *Chem. Phys. Lett.* **1996**, *259*, 669−678.

(56) de Souza, G. L. C.; Peterson, K. A. Probing the ionization potentials of the formaldehyde dimer. *J. Chem. Phys.* **2020**, *152*, No. 194305.

(57) de Souza, G. L. C.; Peterson, K. A. Ionization potentials for the H$_2$CO trimer. *J. Chem. Phys.* **2021**, *155*, No. 084304.

(58) de Souza, G. L. C.; Peterson, K. A. A high level theory investigation on the lowest-lying ionization potentials of glycine (NH$_2$CH$_2$COOH). *Phys. Chem. Chem. Phys.* **2022**, *24*, No. 17751.

(59) Dixon, D. A.; Feller, D.; Peterson, K. A. Chapter one - a practical guide to reliable first principles computational thermochemistry predictions across the periodic table. *Annu. Rep. Comput. Chem.* **2012**, *8*, 1−28.

(60) Matthews, D. A.; Cheng, L.; Harding, M. E.; Lipparini, F.; Stopkowicz, S.; Jagau, T.-C.; Szalay, P. G.; Gauss, J.; Stanton, J. F. Coupled-Cluster Techniques for Computational Chemistry: the CFOUR Program Package. *J. Chem. Phys.* **2020**, *152*, No. 214108.

(61) Tschumper, G. S.; Leininger, M. L.; Hoffman, B. C.; Valeev, E. F.; Schaefer, H. F., III; Quack, M. Anchoring the water dimer potential energy surface with explicitly correlated computations and focal point analyses. *J. Chem. Phys.* **2002**, *116*, 690−701.

(62) Mukhopadhyay, A.; Xantheas, S. S.; Saykally, R. J. The water dimer II: Theoretical investigations. *Chem. Phys. Lett.* **2018**, *700*, 163−175.

(63) Miliordos, E.; Xantheas, S. S. An accurate and efficient computational protocol for obtaining the complete basis set limits of the binding energies of water clusters at the MP2 and CCSD(T) levels of theory: Application to (H$_2$O)$_m$, m = 2−6, 8, 11, 16, and 17. *J. Chem. Phys.* **2015**, *142*, No. 234303.

(64) Dyke, T. R.; Mack, K. M.; Muenter, J. S. The structure of water dimer from molecular beam electric resonance spectroscopy. *J. Chem. Phys.* **1977**, *66*, 498−510.

(65) Lane, J. R. CCSDTQ Optimized Geometry of Water Dimer. *J. Chem. Theory Comput.* **2013**, *9*, 316−323.

(66) Gillan, M. J.; Alfè, D.; Michaelides, A. Perspective: How good is DFT for water? *J. Chem. Phys.* **2016**, *144*, No. 130901.

(67) Krest'yaninov, M. A.; Titova, A. G.; Zaichikov, A. M. Intra- and intermolecular hydrogen bonds in ethylene glycol, monoethanol-

amine, and ethylenediamine. *Russ. J. Phys. Chem. A* **2014**, *88*, 2114−2120.

(68) Kollipost, F.; Otto, K. E.; Suhm, M. A. A Symmetric Recognition Motif between Vicinal Diols: The Fourfold Grip in Ethylene Glycol Dimer. *Angew. Chem., Int. Ed.* **2016**, *55*, 4591−4595.

(69) Loru, D.; Peña, I.; Sanz, M. E. Ethanol dimer: Observation of three new conformers by broadband rotational spectroscopy. *J. Mol. Spectorsc.* **2017**, *335*, 93−101.

(70) Miliordos, E.; Aprà, E.; Xantheas, S. S. Optimal geometries and harmonic vibrational frequencies of the global minima of water clusters $(H_2O)_n$, n = 2−6, and several hexamer local minima at the CCSD(T) level of theory. *J. Chem. Phys.* **2013**, *139*, No. 114302.

(71) de Jong, W. A.; Harrison, R. J.; Dixon, D. A. Parallel Douglas-Kroll energy and gradients in NWChem: Estimating scalar relativistic effects using Douglas-Kroll contracted basis sets. *J. Chem. Phys.* **2001**, *114*, 48−53.

(72) Douglas, M.; Kroll, N. M. Quantum electrodynamical corrections to the fine structure of helium. *Ann. Phys.* **1974**, *82*, 89−155.

(73) Jansen, G.; Hess, B. A. Revision of the Douglas-Kroll transformation. *Phys. Rev. A* **1989**, *39*, No. 6016.

(74) de Souza, G. L. C.; Peterson, K. A. Exploring ground-state and ionization potentials of the $H_2CO\cdots HNO$ dimers. *Phys. Chem. Chem. Phys.* **2025**, *27*, 3854−3860.

(75) Tanaka, H. K.; Prudente, F. V.; Medina, A.; Marinho, R. R. T.; Homem, M. G. P.; Machado, L. E.; Fujimoto, M. M. Photoabsorption and photoionization cross sections for formaldehyde in the vacuum-ultraviolet energy range. *J. Chem. Phys.* **2017**, *146*, No. 094310.

(76) Changala, P. B.; Nguyen, T. L.; Baraban, J. H.; Ellison, G. B.; Santon, J. F.; Bross, D. H.; Ruscic, B. Active Thermochemical Tables: The Adiabatic Ionization Energy of Hydrogen Peroxide. *J. Phys. Chem. A* **2017**, *121*, 8799−8806.

(77) Tomoda, S.; Achiba, Y.; Kimura, K. Photoelectron spectrum of the water dimer. *Chem. Phys. Lett.* **1982**, *87*, 197−200.

(78) Knowles, P. J.; Hampel, C.; Werner, H. J. Coupled cluster theory for high spin, open shell reference wave functions. *J. Chem. Phys.* **1993**, *99*, 5219−5227.